Journal of Cerebral Blood Flow & Metabolism (2015) 35, 319–328

www.jcbfm.com

ORIGINAL ARTICLE

Deciphering of mitochondrial cardiolipin oxidative signaling in cerebral ischemia-reperfusion

Jing Ji[1,2,3,4,5,10], Sophie Baart[1,2,6,10], Anna S Vikulina[3,4], Robert SB Clark[1,2,7], Tamil S Anthonymuthu[1,2,4], Vladimir A Tyurin[3,4], Lina Du[1,2], Claudette M St Croix[3], Yulia Y Tyurina[3,4], Jesse Lewis[1,2], Erin M Skoda[8], Anthony E Kline[9], Patrick M Kochanek[1,2,7], Peter Wipf[8], Valerian E Kagan[3,4] and Hülya Bayır[1,2,3,4,7]

It is believed that biosynthesis of lipid mediators in the central nervous system after cerebral ischemia-reperfusion starts with phospholipid hydrolysis by calcium-dependent phospholipases and is followed by oxygenation of released fatty acids (FAs). Here, we report an alternative pathway whereby cereberal ischemia-reperfusion triggered oxygenation of a mitochondria-specific phospholipid, cardiolipin (CL), is followed by its hydrolysis to yield monolyso-CLs and oxygenated derivatives of fatty (linoleic) acids. We used a model of global cerebral ischemia-reperfusion characterized by 9 minutes of asphyxia leading to asystole followed by cardiopulmonary resuscitation in postnatal day 17 rats. Global ischemia and cardiopulmonary resuscitation resulted in: (1) selective oxidation and hydrolysis of CLs, (2) accumulation of lyso-CLs and oxygenated free FAs, (3) activation of caspase 3/7 in the brain, and (4) motor and cognitive dysfunction. On the basis of these findings, we used a mitochondria targeted nitroxide electron scavenger, which prevented CL oxidation and subsequent hydrolysis, attenuated caspase activation, and improved neurocognitive outcome when administered after cardiac arrest. These data show that calcium-independent CL oxidation and subsequent hydrolysis represent a previously unidentified pathogenic mechanism of brain injury incurred by ischemia-reperfusion and a clinically relevant therapeutic target.

Journal of Cerebral Blood Flow & Metabolism (2015) **35,** 319–328; doi:10.1038/jcbfm.2014.204; published online 19 November 2014

Keywords: cardiac arrest; cardiopulmonary resuscitation; heart arrest; XJB-5-131

INTRODUCTION

Each year cardiac arrest (CA) affects more than 350,000 people in the United States alone. The overall survival rate for out of hospital CA is 9.5% reaching up to 40% for in hospital CA in children.[1] In survivors, functional correlates of neuronal injury emerge as the principal determinant of outcome.[2] An unfavorable neurologic outcome is seen in approximately 50% of the survivors when outcome is reported.[2] Supraphysiologic production of reactive oxygen species (ROS) after reperfusion is implicated as a key contributor to the pathophysiology of CA-induced neurologic injury. Despite the powerful impact of free radical-mediated damage after cerebral ischemia-reperfusion[3,4] and antioxidant therapies showing promise experimentally, clinical trials have failed. Unless the true sources and mechanisms of CA redox imbalance are identified, the use of sacrificial antioxidants and free radical scavengers are apt to fail. Thus, a paradigm-shifting approach is required.

Cessation of oxygen and substrate delivery during CA causes mitochondrial dysfunction and energy depletion.[5] Under energy-deficient conditions, ionic imbalances and activation of NMDA receptors result in overloading of Ca^{2+} ions in neurons.[6,7] This in turn can trigger phospholipase A_2 (PLA_2) activation leading to the accumulation of lysophospholipids and polyunsaturated fatty acids (PUFAs) such as arachidonic and docosohexaenoic acids (AA, DHA).[8] Upon successful resuscitation, the latter can undergo enzymatic oxygenation by cyclooxygenases (COX) and lipoxygenases (LOX) to yield eicosanoids and docosanoids.[9] Delivery of oxygen to dysfunctional mitochondria may be associated with generation of ROS and peroxidation of polyunsaturated phospholipids, particularly cardiolipin (CL), as has been documented for traumatic brain injury.[10] Recently, we discovered that peroxidized CL can be hydrolyzed by mitochondrial Ca^{2+}-independent $iPLA_2\gamma$ and release oxygenated PUFA.[11] Thus, two different pathways—one initiated by Ca^{2+}-dependent PLA_2 with subsequent oxygenation of PUFA by COX and LOX, or the other involving Ca^{2+}-independent CL oxidation by cytochrome c with subsequent hydrolysis by $iPLA_2\gamma$—may result in the production of a variety of lipid mediators after CA (Figure 1). Defining their significance and contribution to the pathogenesis of brain injury has primary importance for mechanism-based selection of therapeutic strategies: inhibitors targeting the COX-LOX pathway versus regulators of CL peroxidation. Here, we report that CA in postnatal day (PND) 17 rats triggered CL oxidation and hydrolysis to generate oxygenated species of linoleic acid and monolyso-CLs in quantitatively comparable amounts. Supression of CL oxidation by a mitochondria targeted nitroxide, XJB-5-131,[12] prevented CL oxidation and hydrolysis, and improved neurocognitive function.

[1]Department of Critical Care Medicine, University of Pittsburgh, Pittsburgh, PA, USA; [2]Safar Center for Resuscitation Research, University of Pittsburgh, Pittsburgh, PA, USA; [3]Department of Environmental and Occupational Health, University of Pittsburgh, Pittsburgh, PA, USA; [4]Center for Free Radical and Antioxidant Health, University of Pittsburgh, Pittsburgh, PA, USA; [5]Department of Neurosurgery, the First Affiliated Hospital of Nanjing Medical University, Nanjing, Jiangsu, China; [6]Medical School at VU Medical Centre, Amsterdam, The Netherlands; [7]Children's Hospital of Pittsburgh, Pittsburgh, PA, USA; [8]Department of Chemistry, University of Pittsburgh, Pittsburgh, PA, USA and [9]Department of Physical Medicine & Rehabilitation, University of Pittsburgh, Pittsburgh, PA, USA. Correspondence: Dr H Bayır, Departments of Critical Care Medicine and Environmental and Occupational Health, University of Pittsburgh, 4401 Penn Avenue, Faculty Pavilion, Pittsburgh, PA 15224, USA.
E-mail: bayihx@ccm.upmc.edu
This work was supported in part by grants from the NIH (NS084604, ES020693, NS076511, U19A1068021, OH008282, NS060005, HD069620).
[10]These authors contributed equally to this work.
Received 16 May 2014; revised 21 October 2014; accepted 22 October 2014; published online 19 November 2014

Thus, Ca^{2+}-independent CL oxidation and subsequent hydrolysis represent a previously unidentified pathogenic mechanism of brain injury incurred by ischemia-reperfusion and a clinically relevant therapeutic target.

MATERIALS AND METHODS

Reagents

Phospholipid and free fatty acid (FFA) standards were purchased from Avanti Polar Lipids Inc. (Alabaster, AL, USA) and from Cayman Chemicals (Ann Arbor, MI, USA) and were of the highest purity available. All other chemicals were purchased from Sigma-Aldrich (St Louis, MO, USA) unless noted otherwise.

Animals

Sprague Dawley PND 17 rats were used for biochemical, behavioral, and pharmacological studies. The institutional Animal Care and Use Committee at the University of Pittsburgh approved the experiments used in this study. The experiments were also conducted in a manner that addressed the key elements of the ARRIVE Guidelines.

Cardiac Arrest Model

Postnatal day 17 male rats underwent CA as described previously.[13] Briefly, rats were randomized to: sham+vehicle, sham+XJB, CA+vehicle, and CA +XJB groups. Rats were anesthetized with 3% isoflurane/50% N_2O/balance oxygen in a plexis glass chamber until unconscious. For surgery, 1% isoflurane/50% N_2O/balance oxygen was used. Rats were tracheally intubated and mechanically ventilated during surgery. Femoral arterial and venous catheters were inserted for monitoring mean arterial pressure, arterial blood sampling and drug administration, respectively. Temperature was maintained at 37°C, monitored by a rectal probe. Vecuronium (1 mg/kg, intravenously) was used for immobilization and was administered 10 minutes before asphyxia. For anesthetic washout, isoflurane/N_2O was discontinued 2 minutes before asphyxia. Rats randomized to CA groups were then disconnected from the ventilator for 9 minutes. Resuscitation was achieved by reconnecting the ventilator, administration of 100% oxygen, manual chest compressions, epinephrine (0.005 mg/kg), and sodium bicarbonate (1 mEq/kg). Heart rate, mean arterial pressure, and arterial blood gas measurements were recorded at baseline, 10, 30, and 60 minutes after resuscitation. Sham animals received the same anesthetics and surgery but no CA. Naïve animals were also used as a control.

Assessment of Phospholipids, Monolysophospholipids, Cardiolipin Oxidation by Liquid Chromatography-Mass Spectrometry

Total lipids were extracted using the Folch procedure from rat cortices. Assessment of phospholipids, monolysophospholipids, and CL oxidation was performed by liquid chromatography-mass spectrometry (LC-MS) utilizing Dionex HPLC system coupled to a LXQTM ion trap MS or to a hybrid quadrupole-orbitrap mass spectrometer, Q-Exactive (ThermoFisher, Inc., San Jose, CA, USA) as described previously.[14–16] For additional detailed analysis of CL and monolyso-CL, normal phase column Luna 3 μm Silica (2) 100 Å column (Phenomenex, Torrance, CA, USA) and gradient solvent A (hexane/propanol/water, 47:57:1, v/v) and solvent B (hexane/propanol/water, 47:57:10, v/v) each containing 5 mmol/L ammonium acetate and 0.01% formic acid was used. The column was eluted at a flow rate of 0.05 mL/min as follows; 0 to 3 minutes, linear gradient,10% to 37% solvent B; 3 to 12.5 minutes, isocratic at 37% solvent B; 12.5 to 20 minutes, linear gradient, 37% to 100% solvent B; 20 to 45 minutes, isocratic at 100% solvent B; 45 to 60 minutes, isocratic at 10% solvent B. For quantitative assessments of CL and monolyso-CL, 1,1′,2,2′-tetramyristoyl-cardiolipin (C14:0)4 and monolyso-CL (C14:0)3 were used as internal standards. 1,1′,2,2′-tetralinoleoyl-cardiolipin (C18:2)4 and monolyso-CL (C18:2)3 were used as reference standards.

Detection of Oxygenated Fatty Acids by Liquid Chromatography-Mass Spectrometry

Oxygenated fatty acid (FA) was analyzed by LC-MS using a LXQTM ion trap mass spectrometer or a hybrid quadrupole-orbitrap mass spectrometer, Q-Exactive. Aliquots of extracted FA (5 μL) were injected into a C_{18} reverse phase column (Luna, 3 μm, 150 × 2 mm) and eluted using gradient solvents (A: tetrahydrofuran/ methanol/water/CH_3COOH, 25:30:50:0.1 (v/v/v/v) and B: methanol/water 90:10 (v/v)) containing 5 mmol/L ammonium acetate at a flow rate of 0.2 mL/min. The column was eluted during first 3 minutes isocratically at 50% B, from 3 to 23 minutes with a linear gradient from 50% solvent B to 98% solvent B, then 23 to 40 minutes isocratically using 98% solvent B, 40 to 42 minutes with a linear gradient from 98% solvent B to 50% solvent B, 42 to 58 minutes isocratically using 50% solvent B for equilibration of the column.

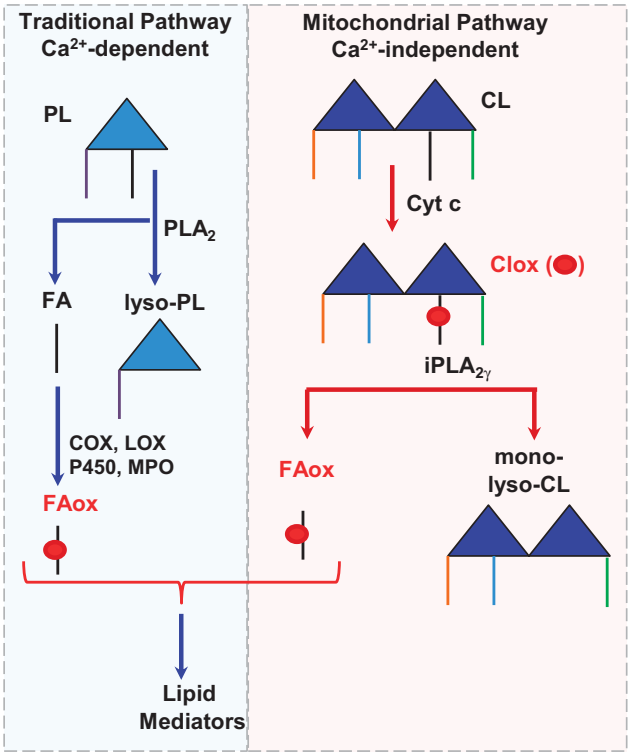

Figure 1. Simplified schema illustrating generation of lipid mediators. In the traditional pathway, Ca^{2+} ions trigger phospholipase A_2 (PLA_2) activation leading to the accumulation of lysophospholipids (lyso-PLs) and polyunsaturated fatty acids (FAs), which can undergo enzymatic oxygenation by cyclooxygenases (COX) and lipoxygenases (LOX) to yield lipid mediators. In the mitochondrial pathway, cytochrome c (cyt c) catalyzes peroxidation of CL, which can be hydrolyzed by mitochondrial Ca^{2+}-independent $iPLA_{2\gamma}$ and release oxygenated polyunsaturated FA (FAox).

Hydrolysis of Cardiolipin by Phospholipases A1 and A2

To identify FA oxidation species, CLs were treated with phospholipase A1 (PLA1) from *Thermomyces lanuginosus* (10 μL/μmol CL) and porcine pancreatic PLA2 (10 U/μmol of CL) in 0.5 mol/L borate buffer, pH 9.0 containing 20 mmol/L cholic acid, 2 mmol/L $CaCl_2$, and 100 μmol/L DTPA for 60 minutes and liberated fatty FA and oxidized FA were extracted by Folch procedure and analyzed by LC-MS. Under these conditions, almost 99% of CLs were hydrolyzed.

XJB-5-131 Treatment

XJB-5-131 was prepared as described.[12,17] For the XJB-5-131 treatment group, XJB-5-131 (10 mg/kg/dose dissolved in 100 μL vehicle) was administered intravenously at 10 minutes and i.p. at 24 hours after the return of spontaneous circulation. Rats in the CA+vehicle and sham +vehicle groups received an equal volume of vehicle (50:50 v/v of cremophor EL ethanol dissolved in 100 μL saline (1:3)).

Assessment of Protein Concentration

Tissue homogenates were briefly sonicated and centrifuged at 10,000 g for 10 minutes. Supernatant was then used for protein measurement using a bovine serum albumin (0.1 mg/mL) standard with a Bio-rad working

reagent (Cat#500-0006, Bio-Rad, Hercules, CA, USA). Absorbance was measured using 595 nm wavelength.

Assessment of Caspase 3/7 Activity

Caspase 3/7 activity was measured using a Caspase-Glo 3/7 assay (Promega, Madison, WI, USA) as previously described.[18] Brain homogenates were briefly sonicated and diluted so that 50 μL sample contained 20 μg of protein. Diluted samples were incubated with the Caspase Glo assay reagent (1:1 volume) for 1 hour. At the end of the incubation period, the luminescent signal was measured using Danatech ML 1000 plate reader and average luminescence per mg protein was calculated. Caspase 3/7 activity was normalized to naïves and expressed as fold increase.

Assessment of Neurobehavioral Outcome

Beam balance and inclined plane tests

The beam balance consisted of placing the rat on an elevated (90 cm) narrow wooden beam (1.5 cm wide) and recording the duration it remains on for a maximum of 60 seconds. Subjects were pretrained on the beam balance 1 day before surgery and assessed on the day of surgery to determine baseline performance. Postoperative testing occurred on days 1 to 5 and consisted of providing three trials (60 seconds allotted time) per day. The average daily scores for each subject were used in the statistical analyses. For the inclined plane, rats were placed on a flat board with increasing angles (45° to 80°). The maximum angle at which the animal could maintain its position for 10 seconds was recorded and used in the statistical analyses.

Assessment of Neurocognitive Outcome

Morris water maze. Spatial memory acquisition and retention were assessed using a Morris water maze task. The maze consisted of a plastic pool (180 cm diameter; 60 cm high) filled with water (26 ± 1°C) to a depth of 28 cm and was situated in a room with salient visual cues that remained constant throughout the study. The platform was a clear Plexiglas stand (10 cm diameter, 26 cm high) and was positioned 26 cm from the maze wall in the SW quadrant and held constant throughout the study for each animal. On days 7 to 9 after CA, the visible platform task (platform raised 2 cm above the water level) was used as a control for potential non-specific deficits (i.e., visual impairments) and motor functions. Acquisition of spatial learning was conducted on postoperative days 10 to 13 and consisted of providing a block of four daily trials to locate the platform when it was submerged 2 cm below the water surface (i.e., invisible to the rat). For each daily block of trials, the rats were placed in the pool facing the wall at each of the four possible start locations (North, East, South, and West) in a randomized manner. Each trial lasted until the rat climbed onto the platform or until 120 seconds had elapsed, whichever occurred first. Rats that failed to locate the goal were manually guided to it where they remained for 30 seconds before being placed in a heated incubator between trials (4-minute intertrial interval). The data used in the statistical analyes consisted of distance traveled (cm) and were obtained using a a video tracking system (AnyMaze, Stoelting, Wood Dale, IL, USA).

Assessment of the Effect of XJB-5-131 on the Enzymatic Activity of Lipoxygenases and Cyclooxygenases

In all, 20 μmol/L of Lineloic acid (LA) was incubated with 5 milliunits of recombinant mouse LOX-12 in 0.1 mol/L Tris-HCl buffer of pH 7.5 containing 5 mmol/L EDTA and 0.03% Tween-20 for 30 minutes with various concentrations (0.1, 1, and 10 μmol/L) of XJB-5-131 and LOX inhibitor Licofelone (10 μmol/L). For COX-1 and COX-2 enzymes, the reaction was conducted in buffer containing 0.1 mol/L Tris-HCl, pH 8.0, 5 mmol/L EDTA, 1 μmol/L Heme and the inhibitor used was piroxicam (10 μmol/L). The reaction was stopped by adding 0.1 mol/L HCl and the LA and oxidized LA were extracted by Folch procedure and analyzed by LC-MS. The LC-MS method was essentially the same as the one that was previously described, with the exception of using a smaller column of 1 mm internal diameter × 150 mm length with a 50-μL/min flow rate.

In Vitro Oxygen Glucose Deprivation

Primary cortical neuronal culture was performed as previously described.[18] For oxygen glucose deprivation (OGD) in neurons, Neurobasal medium and B27 supplements (Life Technologies, Carlsbad, CA, USA) were removed and replaced with custom-made medium lacking sodium pyruvate and L-aspartate with a final concentration of 0.5 mmol/L D-glucose and 2 mmol/L L-glutamine, and they were placed into a pre-warmed Billups-Rothenberg modular incubator chamber containing 50 mL of sterile distilled-deionized water at 37 °C. The chamber was flushed with 95% argon and 5% CO_2 for 15 minutes and then sealed. The chamber was then placed in an incubator at 37 °C for 1 hour. Afterwards cultures were returned to the incubator containing 95% air and 5% CO_2.

Assessment of Mitochondrial Superoxide Production with MitoSOX

The mitochondrial superoxide production was measured by flow cytometry and dual excitation wavelength (395 and 508 nm) live cell imaging as described.[19,20] Briefly, MitoSOX Red (Life Technologies) was added to the neuronal cultures at a final concentration of 5 μmol/L. The cells were detached with 0.1% trypsin-EDTA at 37°C for 5 minutes, washed twice with PBS and then spun down at 600 *g* at 4°C for 5 minutes. The cells were then incubated on ice for 30 minutes to allow loading of MitoSOX Red. The cells were washed two times with PBS and placed in a sterile FACS tube at a concentration of 3 to 5×10^6 cells per 100 μL until the samples were analyzed *via* flow cytometer (Becton-Dickison, Franklin Lakes, NJ, USA). Hoechst 33258 (1 μg/mL; Life Technologies) was added 1 minute before flow-cytometer analysis. For dual excitation wavelength live cell imaging, cells were seeded on 40 mm coverglass and incubated with the superoxide indicator MitoSOX Red (5 μmol/L, Invitrogen, Eugene, OR, USA) for 15 minutes at 37°C. Cells were then washed with PBS, the media replaced and the dish inserted in a closed, thermo-controlled (37°C) stage top chamber (FCS2, Bioptechs Inc., Butler, PA, USA) atop the motorized stage of an inverted Nikon TiE fluorescent microscope (Nikon Inc., Melville, NY, USA) equipped with a × 60 oil immersion optic (Nikon, CFI PlanFluor, NA 1.43) and NIS Elements Software. MitoSOX Red was excited using a Lumencor diode-pumped light engine (SpectraX, Lumencor Inc., Beaverton, OR, USA) at 395 and 508 nm and emissions were detected using a longpass filter set (Chroma Technology Corp., Bellows Falls, VT, USA) and ORCA-Flash 4.0 sCMOS camera (HAMAMATSU Corporation, Bridgewater, NJ, USA). Data were collected in 10 to 20 cells per stage position, with 10 stage positions in each experiment.

Statistical Analysis

The motor and cognitive data were analyzed by repeated-measures analysis of variance (RM-ANOVA) using Statview 5.0.1 software (Abacus Concepts, Inc., Berkeley, CA, USA). When the overall ANOVA revealed a significant effect, the data were further analyzed with the Bonferroni/Dunn *post hoc* test to determine specific group differences. The behavioral data are presented as the mean ± s.e.m. and are considered as significant when the corresponding *P*-values are less than 0.05 or as determined by the Bonferroni/Dunn statistic after adjusting for multiple comparisons. All other data were expressed as mean ± s.d. Statistical comparisons between groups were performed by ANOVA for biochemical assessments. When the overall ANOVA revealed a significant effect, the data were further analyzed with the Tukey *post hoc* test to determine specific group differences. Differences were considered as statistically significant when the *P*-value was less than 0.05 and are indicated in figure legends.

RESULTS

We performed full LC-MS analysis of six major classes of phospholipids in PND17 rat cortex—phosphatidylcholine (PC), phosphatidylethanolamine (PE), phosphatidylserine (PS), phosphatidylinositol (PI), phosphatidylglycerol (PG), and CL (Figure 2A). Molecular speciation of phospholipid classes corresponded to the previously published data.[10] While CA did not cause large changes in either molecular speciation or levels of individual phospholipids, detailed analysis of lysophospholipis (Figure 2B) revealed accumulation of monolyso-CL (Figure 2C). Other classes of lysophospholipids did not undergo statistically significant increases (Figure 2C). We further performed a more detailed analysis of CLs and their hydrolysis products (Figures 3A to 3C). Lyso-CLs were grouped into four major clusters (Figure 3A). The contents of all detected lyso-CL species were increased after CA

A

PL	*Naive*	*CA*	*CA/XJB*
	nmol/mg protein ± SD		
PC	229±12	237±36	236±33
PE	73±8	78±7	74±10
PS	31±5	32±5	31±7
PI	8±2	10±2	8±2
PG	14±2	15±2	13±1
CL	9.0±1.2	9.3±0.9	8.2±1.3

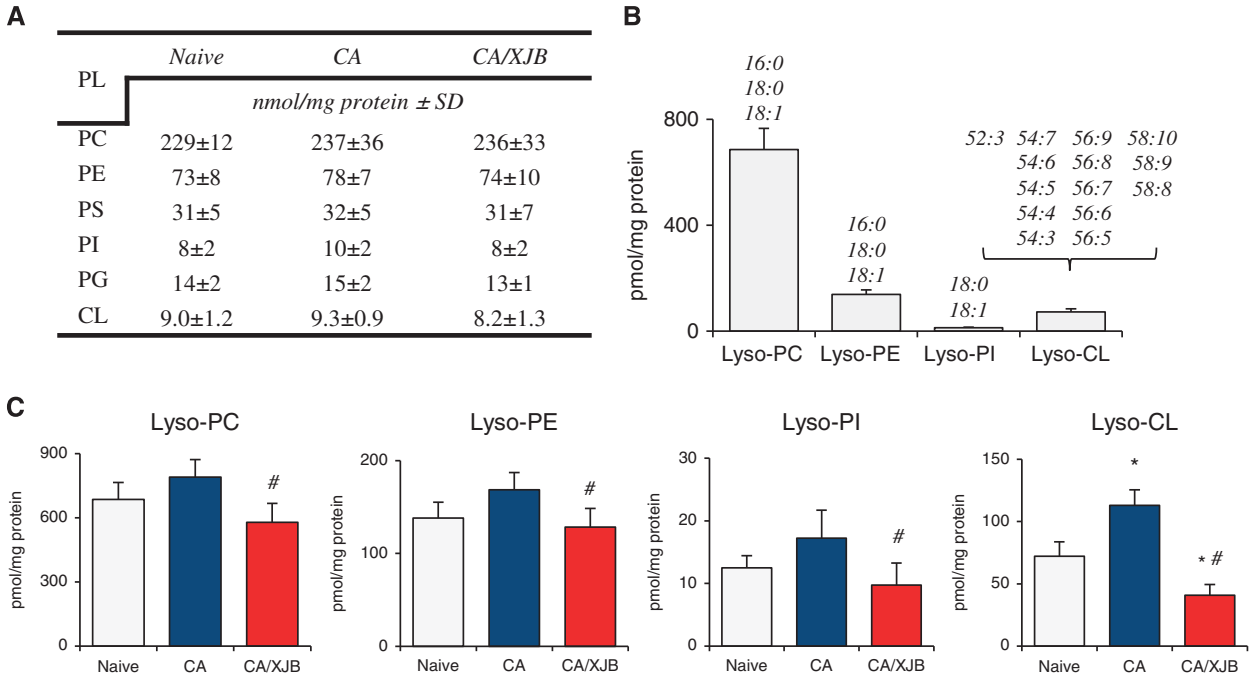

Figure 2. Quantification of cortical phospholipids and lyso-phospholipids (PLs) after cardiac arrest (CA). (**A**) The levels of individual phospholipids (phosphatidylcholine (PC), phosphatidylethanolamine (PE), phosphatidylserine (PS), phosphatidylinositol (PI), phosphatidylglycerol (PG) and cardiolipin (CL)) did not change after CA. (**B**) Major molecular species of lysophospholipids. (**C**) CA-induced accumulation of lyso-CL. Other lyso-PLs did not undergo a statistically significant increase. XJB-5-131 decreased levels of lyso-PLs. Lyso-PA and lyso-PS were not detected. $^{*}P < 0.05$ versus naive; $^{\#}P < 0.05$ versus CA, mean ± s.d., $n = 4$/group.

(Figure 3B). Given that CL is a mitochondria-specific phospholipid, these results indicate that CA-dependent hydrolytic events were localized predominantly to mitochondria rather than randomly affecting all intracellular membranes and organelles.

We found that CA did not cause significant changes in the content of the major oxidizable polyunsaturated FFA: LA [C18:2, octadecaenoic acid], AA [C20:4], and DHA [C22:6]. In contrast, the amounts of oxidized polyunsaturated FFA (FFAox) were increased after CA exclusively at the expense of LA (Figure 4A). The species of peroxidized LA were identified as hydroxyoctadecadienoic acid (HODE), epoxyoctadecenoic acid (EpOME), and hydroperoxyoctadecenoic acid (HpODE). Further evaluation by chromatographic separation and MS/MS analysis identified HODEs as 13- and 9-HODE and EpOMEs as 12(13)- and 9(10)-EpOME (Figure 4B). A comparison of CA-induced accumulation of oxygenated species of LA with the total amounts of lysophopspholipids revealed quantitative correspondence as well as a significant difference versus control values (Figure 4C). These comparisons suggest that oxidized C18:2 residues were the most predominant substrates of endogenous PLA_2-dependent hydrolysis triggered by CA. Moreover, mitochondrial CL species with peroxidized C18:2 residues represented the major substrates of hydrolytic attack. Some of the endogenously accumulated CLox species formed after CA remained non-hydrolyzed as we were able to detect them (as non-hydrolyzed CLox species) in some of the cortical samples (Figures 5A and 5B).

Assuming that CL oxidation preceded its hydrolysis to monolyso-CL and oxidized LA, we chose to use an inhibitor of CL oxidation, XJB-5-131, which had been shown to effectively prevent CL oxidation after traumatic injury *in vivo*.[18] Indeed, we found that XJB-5-131 treatment significantly decreased levels of lyso-CLs and oxygenated LA versus vehicle (Figures 2C, 4A and 4C). Given that XJB-5-131 was able to suppress CL oxidative metabolism induced by CA, we were further interested in testing its therapeutic potential. We focused our efforts on the ability of XJB-5-131 to attenuate CA-induced caspase 3/7 activation and neurocognitive dysnfunction. Caspase 3/7 activity in cortex and cerebellum was increased ~10-fold at 24 hours but not at 3 hours after CA compared with controls (Figures 6A and 6B). This increase in caspase 3/7 activity at 24 hours was attenuated by XJB-5-131 (Figures 6A and 6B).

To evaluate the effect of XJB-5-131 on ischemia reperfusion-induced mitochondrial ROS generation, we evaluated MitoSOX response by flow cytometry in primary cortical neurons exposed to 1 hour of OGD and 2 and 24 hours of reperfusion. Mitochondrial ROS generation was increased after reperfusion. Mitochondria-targeted XJB-5-131 was effective in attenuating ROS generation (Figure 7A). Analysis by dual excitation wavelength live cell imaging for detection of hydroxy-mito-ethidium identified the mitochondrial ROS that are generated after ischemia reperfusion as superoxide (Figure 7B).

We next performed neurobehavioral and neurocognitive testing on PND 17 rats subjected to CA. We assessed motor function with the well-established beam balance and inclined platform tests and evaluated cognitive performance using Morris water maze task, which are sensitive to motor and cognitive dysfunction after CA.[21] There were no statistically significant differences between the two sham groups thus they were pooled into one group for analysis. Balancing ability or inclined platform performance did not differ among groups before surgery (Figures 8A and 8B). After CA, a significant impairment in both the beam balance and inclined plane tasks was observed on day 1, with recovery in motor function observed in both tasks by day 3. Accelerated recovery of motor function (in both tasks) was observed in the CA+XJB group compared with the CA+vehicle group (Figures 8A and 8B).

No significant difference was observed among the groups during the visible platform task on postoperative days 7 to 9 as all groups became increasingly better at reaching the platform as shown by shorter swim distances. During the spatial acquisition phase (hidden platform), the RM-ANOVA revealed a significant difference among groups. Subsequent *post hoc* analyses showed that the sham group performed significantly better than the CA +vehicle group, as evidenced by substantially shorter swim

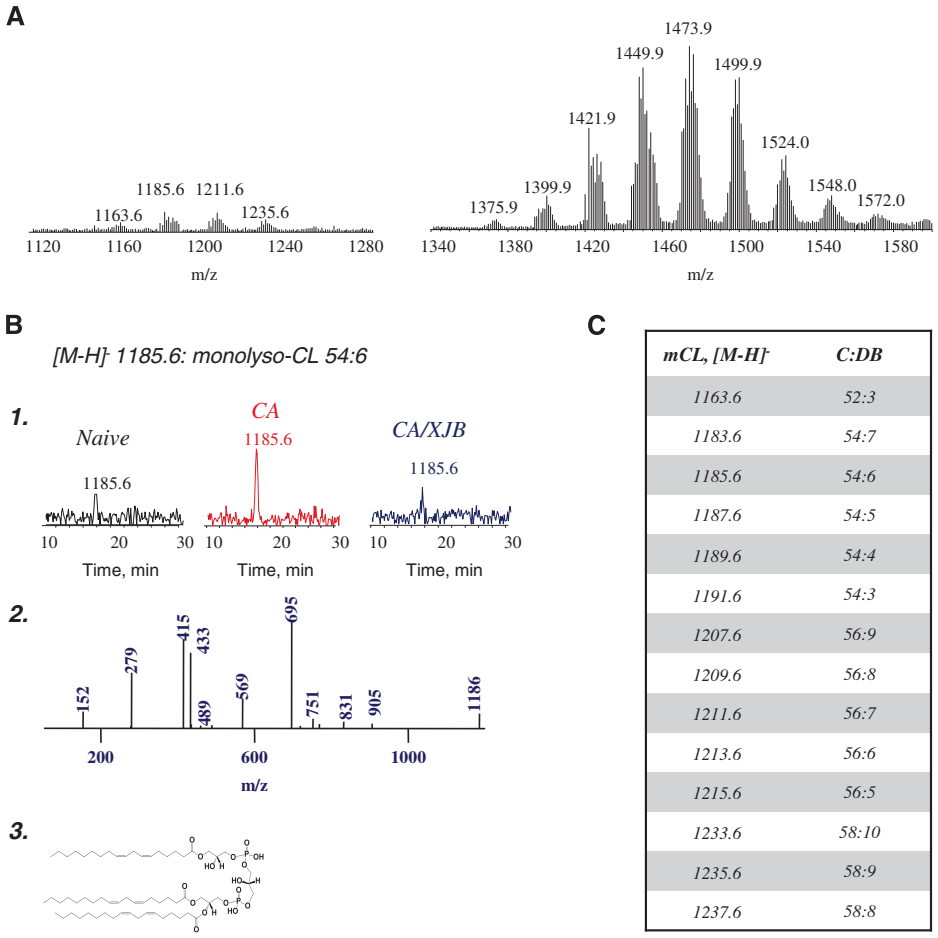

mCL, [M-H]-	*C:DB*
1163.6	*52:3*
1183.6	*54:7*
1185.6	*54:6*
1187.6	*54:5*
1189.6	*54:4*
1191.6	*54:3*
1207.6	*56:9*
1209.6	*56:8*
1211.6	*56:7*
1213.6	*56:6*
1215.6	*56:5*
1233.6	*58:10*
1235.6	*58:9*
1237.6	*58:8*

Figure 3. Analysis of cardiolipins (CLs) and their hydrolysis products in cortex. (**A**) Typical MS^1 spectra of CLs (right) and monolyso-CLs (left). (**B**) (1) Typical liquid chromatography-mass spectrometry (LC-MS) profiles for one of the major lyso-CLs [M-H]- (m/z 1185.6) from naïve, CA, and CA+XJB; normal phase HPLC/ESI-MS. (2) MS^2 spectrum of lyso-CL 54:6 in cortex after CA; normal phase HPLC-ESI-MS. (3) Structure of lyso-CL 54:6 (18:2/18:2/18:2). (**C**) Major molecular species of monolyso-CLs identified after CA in cortex (C:DB—number of carbon atoms to double bonds in fatty acid chains).

distances, but did not differ from the CA+XJB group. Moreover, the CA+XJB group swam significantly shorter distances to the platform relative to the CA+vehicle group on postoperative days 12 and 13 (Figure 8C). There were no statistical differences in swim speeds among the groups.

DISCUSSION

Mitochondria are crucial in life in that they synthesize ATP, providing the cell with energy. However during reperfusion after CA, damaged brain mitochondria: (1) produce toxic-free radicals that directly attack vital cellular constituents;[22] (2) are at the convergence of critical cell death pathways such as apoptosis and necrosis;[14] and (3) are powerful mediators of inflammation.[23] Central to all three of these potentially pathologic mechanisms is the supraphysiologic generation of ROS, which can be used for oxidative signaling by selective enzymatic oxidation of CL followed by its hydrolysis and generation of lyso-CL and oxidized LA. This pathway is separate and distinct from the tradional understanding of the role of ROS. We present evidence that supression of this pathway by a mitochondria targeted inhibitor of CL oxidation improves outcome after CA.

During CA, cessation of blood flow and interruption of delivery of oxygen and other essential metabolites results in increased levels[6,7] of Ca^{2+} and activation of of Ca^{2+}-dependent PLA_2 leading to hydrolysis and release of PUFA esterified into cellular phospholipids.[16] Upon reperfusion, the released PUFA can be used as substrates for oxygenation reactions catalyzed by several groups of cytosolic enzymes—COX, LOX, different cytochrome P450 isoforms, and peroxidases.[16] The major sources of phospholipids for Ca^{2+}-dependent PLA_2-mediated FA hydrolysis are PE, PC, and PS of plasma and intracellular membranes with simultaneous accumulation of lysoPE, lysoPC, and lysoPS, respectively.[16] Previous work in focal cerebral ischemia showed that activation of Ca^{2+}-dependent PLA_2 generates oxygenated AA and DHA derivatives in the brain.[24] Furthermore, prostaglandins and cyclopentenone prostaglandins are generated by COX-2 at 24 hours after CA in immature brain.[25] The late appearance of mediators from AA oxygenation could be related to the postischemic inflammatory response after global cerebral ischemia.[26]

Alternatively, reperfusion-associated oxidation of phospholipids could produce their modified forms that might be metabolized by Ca^{2+}-*independent* phospholipases, for example by $iPLA_2\gamma$ in mitochondria. A specific feature of this pathway may be its selectivity toward a peroxidizable and subsequently hydrolyzable phospholipid substrate, a unique phospholipid of mitochondria, CL.[27,28] It was reported that $iPLA_2\gamma$ is responsible for hydrolysis of CL and accumulation of monolysoCL in Barth syndrome and hypertensive heart failure.[27,28] We were able to detect significant accumulation of monolyso-CL species after CA whereas the production of other lyso-

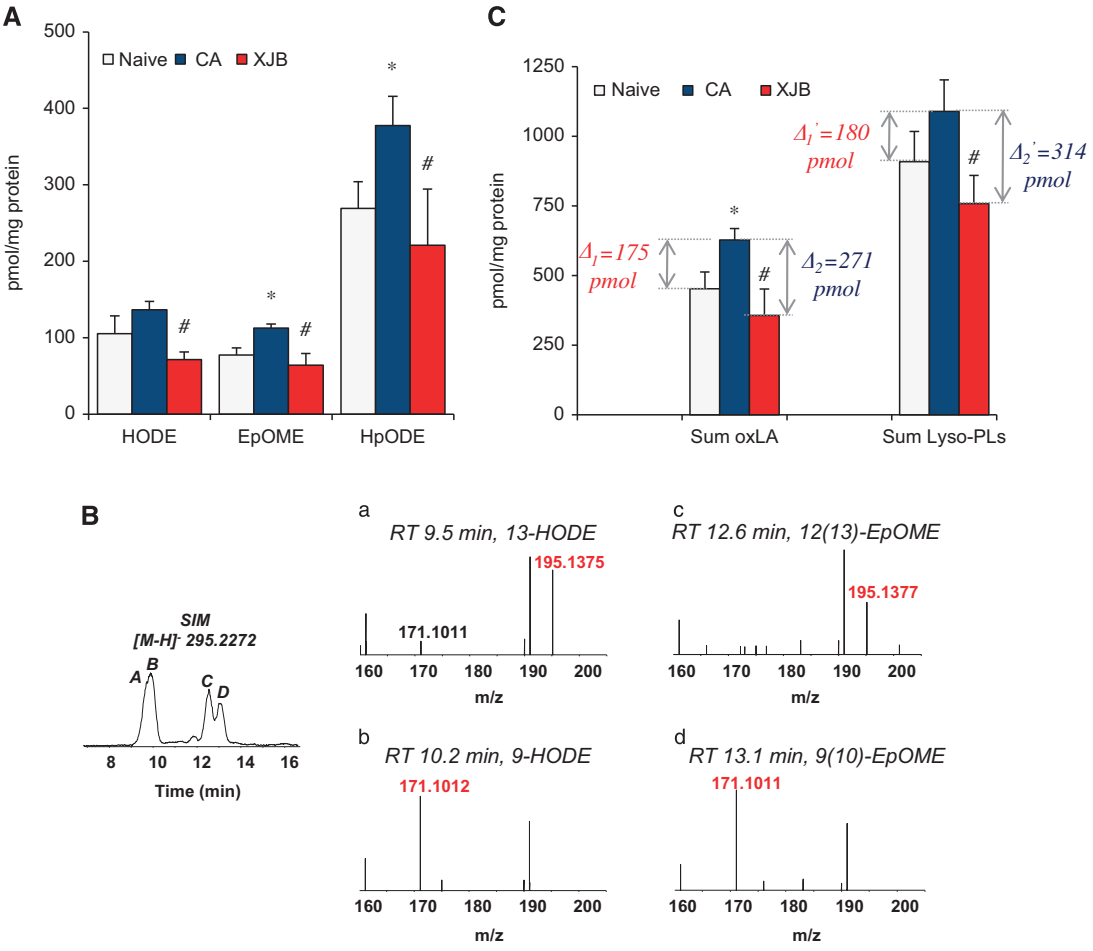

Figure 4. Quantitative assessment of oxidized polyunsaturated free fatty acids (FFAox) in cortex. (**A**) The amounts of FFAox were increased after cardiac arrest (CA) exclusively at the expense of C18:2 (linoleic [or octadecaenoic] acid). The detected species of peroxidized C18:2 were identified as hydroxyoctadecadienoic (HODE), epoxyoctadecenoic (EpOME), and hydroperoxyoctadecenoic acid (HpODE). The amount of oxidized C18:2 species decreased by XJB-5-131 treatment after CA. $^{*}P < 0.01$ versus naive; $^{\#}P < 0.01$ versus CA vehicle. Mean ± s.d., $n = 4$/group. (**B**) Further evaluation by chromatographic separation and MS^2 analysis identified HODEs as 13- and 9-HODE (a, b) and EpOMEs as 12 (13)- and 9(10)-EpOME (c, d). (**C**) Contents of total lysophospholipids (lyso-PLs) and free oxidized linoleic acid (oxLA) in cortex. Mean ± s.d., $n = 4$/group. Δ_1—the difference between CA and naïve samples (pmol/mg protein); Δ_2—the difference between CA and CA+XJB samples (pmol/mg protein). $^{*}P < 0.05$ versus naïve; $^{\#}P < 0.05$ versus CA.

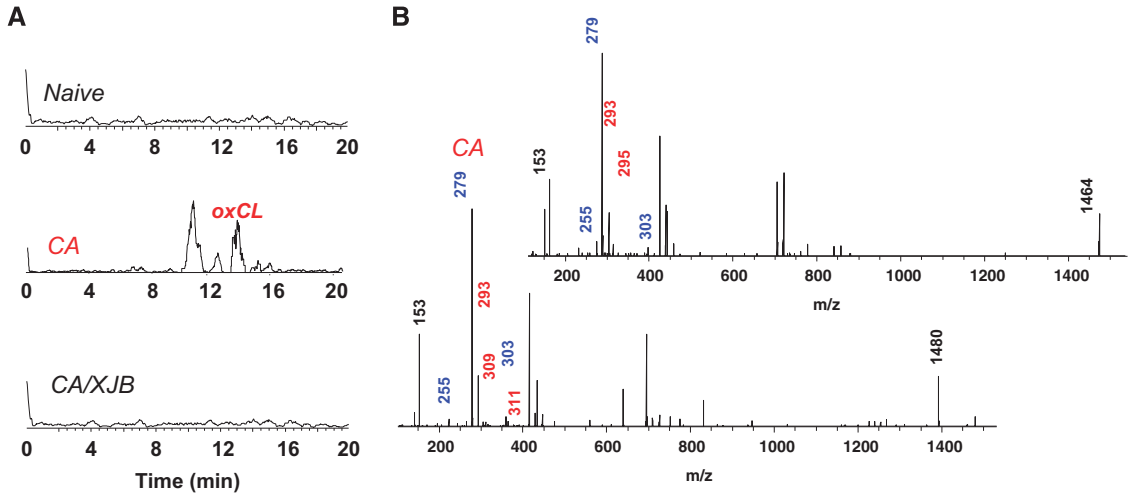

Figure 5. Analysis of oxidized cardiolipin (oxCL) in cortex. (**A**) Typical liquid chromatography-mass spectrometry (LC-MS) profiles of oxCL in naïve, CA, and CA+XJB. (**B**) MS^2 spectra of CL [M-H]- 1464 (top) and 1480 (bottom) after cardiac arrest (CA); characteristic ions with m/z 293, 295, 309, and 311 are marked with red.

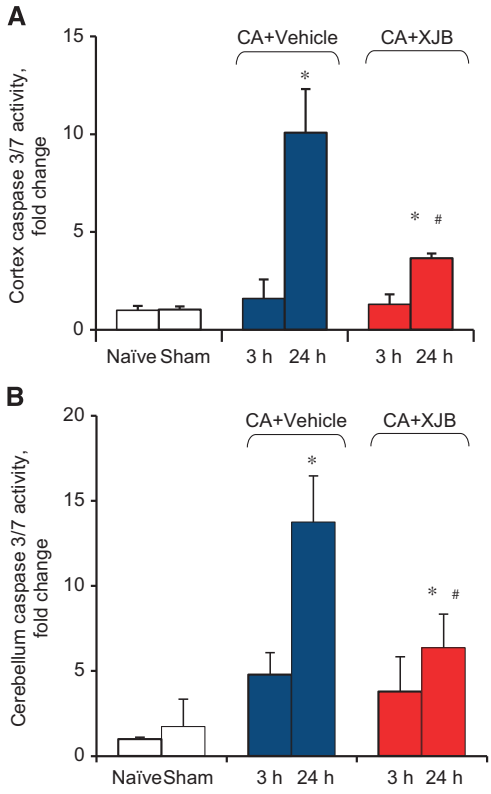

Figure 6. Quantification of caspase 3/7 activity in postnatal day (PND) 17 rats. Caspase 3/7 activity was increased in cortex (**A**) and cerebellum (**B**) at 24 hours after cardiac arrest (CA) versus naïve and sham controls. XJB-treated animals showed decreased caspase 3/7 activity compared with vehicle group. $^{*}P < 0.05$ versus naïve, $^{\#}P < 0.05$ versus CA+vehicle, Mean ± s.d., $n = 5$ for sham, $n = 4$ for other groups.

phospholipids—lyso-forms of PE, PC, and PS, did not reach significance. This might suggest that mitochondrial events dominated in early CA-triggered pathogenic pathways. The selectivity of CA-induced CL modification is surprising given that CL constitutes only a small fraction (~2 mol%) of all brain phospholipids.[10] Quantitative correspondence of lyso-CLs and FFAox suggests that oxidized CLs were the major substrates of PLA_2-catalyzed hydrolysis and release of these products. This is further supported by data showing that only small amounts of FFAox were detected when lipid extracts were hydrolyzed by a mixture of exogenously added PLA_1+PLA_2 (Figure 9).

These observations prompted us to use a mitochondria-targeted electron scavenger, XJB-5-131, as a protective therapeutic modality. We have previously shown that XJB-5-131 partitions into and accumulates almost exclusively in mitochondria such that it is not detectable in cytosol (e.g., by electron paramagnetic resonance spectroscopy).[18] A fluorescently labeled analog of XJB-5-131—BODIPY-FL-XJB-5-131—colocalizes with mitochondria labeled with Mito-tracker (Figure 7A). We found that XJB-5-131 was effective in attenuating both the production of monolyso-CL and the release of lipid mediators and the biochemical and behavioral impairments induced by CA. We found that lyso-CL levels were lower in XJB-treated CA rats compared with naives. An array of diversified lipid mediators derived from PUFA have central roles in cellular signaling in central nervous system.[8] The conventional mechanisms for their production are associated with cytosolic enzymatic machinery.[8] Recently, we identified mitochondrial CLs as a new source of lipid mediators in the brain whereby peroxidation of CL by cytochrome c, formation of CLox and its subsequent hydrolysis resulted in the accumulation of lyso-CLs and FFAox (lipid mediators).[11] It is possible that this novel pathway is involved in normal signaling processes originating in mitochondria and is exacerbated during ischemia-reperfusion injury. If this assumption is correct, then by scavenging electrons XJB-5-131 will prevent the dismutation of $O_2^{\bullet -} \rightarrow H_2O_2$ hence limit the generation of CLox by the peroxidase activity of cytochrome

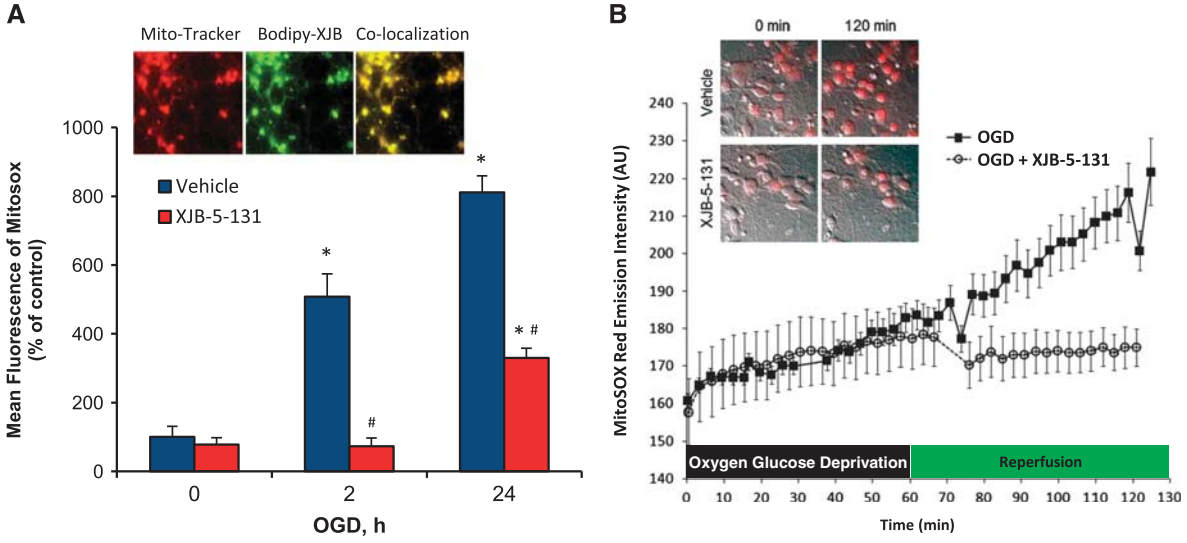

Figure 7. Assessment of mitochondrial superoxide generation in primary cortical neurons after oxygen glucose deprivation (OGD). (**A**) Quantitative analysis of mitochondrial reactive oxygen species (ROS) generation by flow cytometry. OGD increased ROS formation in neuronal mitochondria at 2 and 24 hours after reperfusion compared with control. XJB-5-131 attenuated OGD-induced mitochondrial ROS generation at both 2 and 24 hours after OGD. $^{*}P < 0.05$ versus 0 hour, $^{\#}P < 0.05$ versus vehicle, Mean ± s.d., $n = 3$/group. Inset: a fluorescently labeled analog of XJB-5-131—BODIPY-XJB-5-131—colocalizes with mitochondria labeled with mitotracker. (**B**) Dual wavelength imaging for superoxide-dependent hydroxylation of mitohydroethidine (HE) to mitoHO-Et+. XJB-5-131 prevented the typical increase in 2-HO-MitoSox seen upon reperfusion after 60 minutes of OGD.

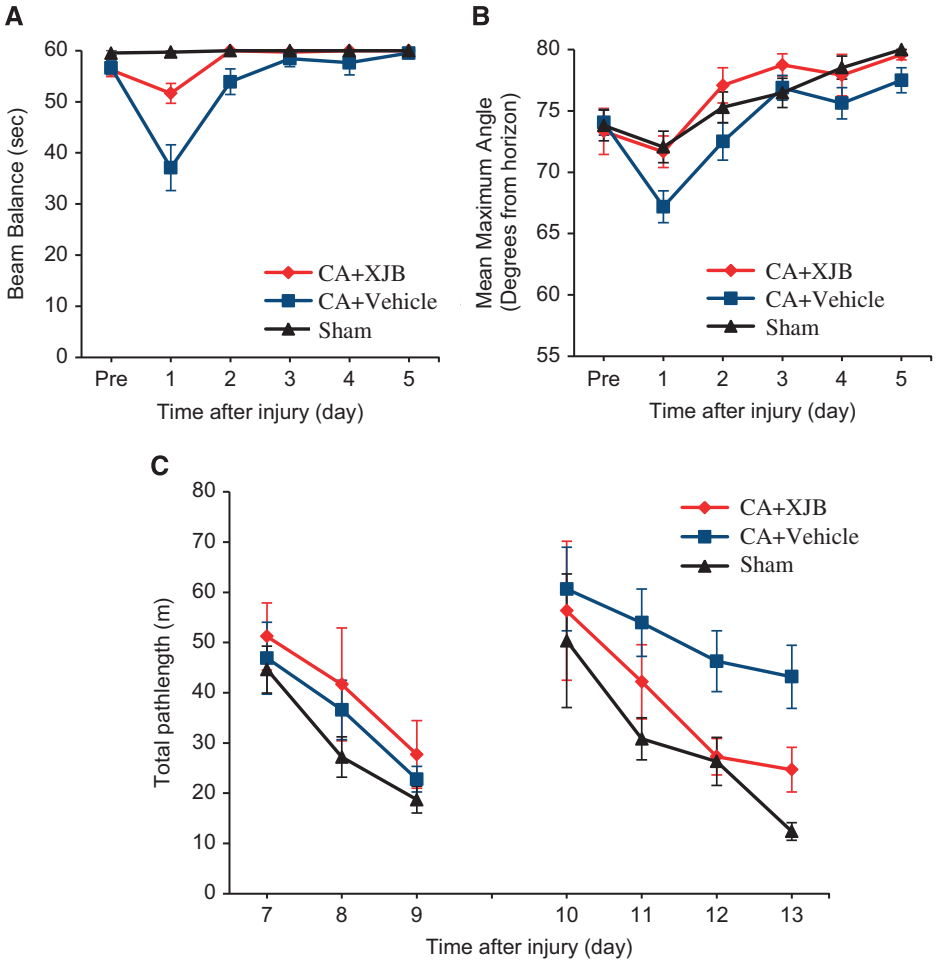

Figure 8. Assessment of neurobehavioral outcome in postnatal day (PND) 17 rats after cardiac arrest (CA). (**A**) Ability of rats to remain on the beam balance apparatus before and after CA or sham insult. Repeated-measures analysis of variance (RM-ANOVA) revealed a significant group ($F_{2,42} = 10.768$, $P = 0.0002$), day ($F_{5,210} = 23.324$, $P < 0.0001$), and group-by-day interaction effect ($F_{10,210} = 10.604$, $P < 0.001$). *Post hoc* analyses revealed that CA+XJB group performed significantly better than CA+vehicle ($P = 0.0009$), but did not differ from the sham control ($P = 0.103$). (**B**) Maximum angle (degrees) for rats to remain on an inclined platform. RM-ANOVA revealed significant day difference among groups ($F_{5,42} = 29.979$, $P < 0.0001$). *Post hoc* analyses revealed that CA+XJB group performed significantly better than the CA+vehicle group ($P = 0.0047$) and did not differ from the sham controls ($P = 0.669$). (**C**) Mean distance (cm) to reach the visible (days 7 to 9) and hidden (days 10 to 13) platform in the Morris water maze (MWM). The RM-ANOVA did not reveal a significant group difference in the visible platform test ($F_{2,42} = 1.174$, $P = 0.319$), suggesting that visual acuity was intact in all rats. In contrast, for the hidden platform test, the RM-ANOVA revealed a significant group ($F_{2,42} = 4.935$, $P = 0.0119$) and day difference ($F_{3,126} = 11.047$, $P < 0.0001$). Subsequent *post hoc* analyses revealed that the CA +XJB group performed significantly better than the CA+vehicle on postoperative days 12 and 13 ($P = 0.0166$ and $P = 0.0084$, respectively), but did not differ from the sham controls ($P > 0.05$). All values are mean ± s.e.m., $n = 12$ to 17 rats per group.

c/CL complex. Consequently, the hydrolysis of CLox and the production of lyso-CL and FFAox will be also suppressed. Liquid chromatography-mass spectrometry analysis of LA oxidation products showed that XJB-5-131 had minimal or no inhibitory effect on the enzymatic activity of COX-1, COX-2, and 12-LOX toward LA, i.e., the fatty acid found to be the major oxygenated product after CA in our study. These data show that the mitochondria-targeted nitroxide, XJB-5-131, is unlikely to have an effect on the traditional pathway of lipid mediator synthesis (Supplementary Figures S1). Taken together, our findings suggest that reperfusion-triggered Ca^{2+}-independent peroxidation reactions likely contribute to CA-associated injury. These results suggest a paradigm shift in our understanding of lipid peroxidation after CA-induced cerebral ischemia-reperfusion.

We have previously shown that CL oxidation has a pivotal role in the mitochondrial stage of the execution of the apoptotic cell death program.[29] During apoptosis, CL interacts with cytochrome c to form a peroxidase complex that catalyzes CL oxidation. Oxidized CL is required for the release of pro-apoptotic factors, including cytochrome c. The latter in turn becomes a part of the caspase activating apoptosome complex.[29] Prevention of this chain of events from occurrence protects against neuronal death.[18,30] Several important features of mitochondrial CL peroxidation after CA should be noted: (1) the degree of oxidized CL accumulation was smaller than observed in experimental traumatic brain injury where ischemia/reperfusion is not predominant; (2) lysoCLs were the main lysophospholipids observed; and (3) LA residues were the primary targets of oxidation. Surprisingly, oxidation products of AA and DHA were not observed in CL at 3 hours after reperfusion. In line with our findings, studies in canine ventricular fibrillation CA showed formation of LA oxidation products, primarily 9- and 13-HODE, generated from both FFA and phospholipids in cortex at 10 minutes and 2 hours after reperfusion.[31] Linoleic acid oxidation products have cytotoxic properties[32] and modulate inflammatory response.[33]

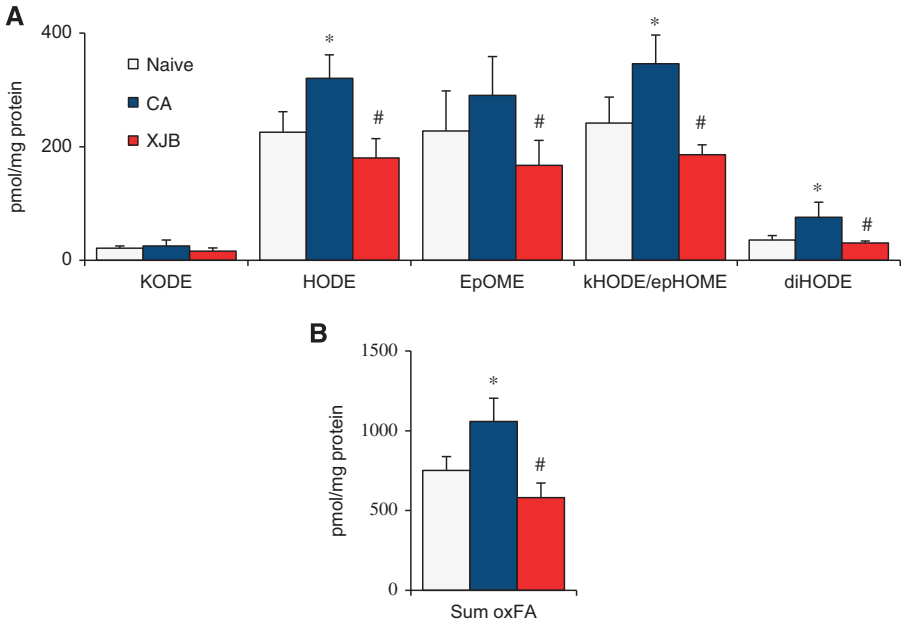

Figure 9. Analysis of nonhydrolyzed oxidized phospholipids. (**A**) Amounts of oxidized fatty acids (FAox) liberated from cortical total lipid extracts by phospholipase A1 (PLA1) plus phospholipase A2 (PLA2) treatment. KODE, ketoooctadecadienoic acid; HODE, hydroxyoctadecadienoic acid; EpOME, epoxyoctadecenoic acid; kHODE, oxo-hydroxyoctadecadienoic acid; epHOME, epoxy-hydroxyoctadecenoic acid; diHODE, dihydroxyoctadecadienoic acid. (**B**) Sum of all oxidized octadecadienoic (linoleic) acid (sum oxLA). $^{*}P < 0.01$ versus naive; $^{\#}P < 0.01$ versus cardiac arrest (CA). Mean ± s.d., $n = 4$/group.

In summary, our study identified a novel alternative source of lipid mediators from CLs after global cerebral ischemia induced by a clinically relevant model of CA. A mitochondria targeted nitroxide electron scavenger, which prevented CL oxidation and hydrolysis, attenuated neuronal death and improved cognitive outcome after CA. This study also reveals that there are additional therapeutic opportunities targeting Ca^{2+}-independent $iPLA_2$ for improving outcome after global cerebral ischemia reperfusion injury.

DISCLOSURE/CONFLICT OF INTEREST

The authors declare no conflict of interest.

REFERENCES

1 Morrison LJ, Neumar RW, Zimmerman JL, Link MS, Newby LK, McMullan PW, Jr. *et al.* Strategies for improving survival after in-hospital cardiac arrest in the united states: 2013 consensus recommendations: A consensus statement from the american heart association. *Circulation* 2013; **127**: 1538–1563.
2 Moler FW, Meert K, Donaldson AE, Nadkarni V, Brilli RJ, Dalton HJ *et al.* In-hospital versus out-of-hospital pediatric cardiac arrest: A multicenter cohort study. *Crit Care Med* 2009; **37**: 2259–2267.
3 Traystman RJ, Kirsch JR, Koehler RC. Oxygen radical mechanisms of brain injury following ischemia and reperfusion. *J Appl Physiol* 1991; **71**: 1185–1195.
4 Siesjo BK, Agardh CD, Bengtsson F. Free radicals and brain damage. *Cerebrovasc Brain Metab Rev* 1989; **1**: 165–211.
5 Han F, Da T, Riobo NA, Becker LB. Early mitochondrial dysfunction in electron transfer activity and reactive oxygen species generation after cardiac arrest. *Crit Care Med* 2008; **36**: S447–S453.
6 Santos MS, Moreno AJ, Carvalho AP. Relationships between atp depletion, membrane potential, and the release of neurotransmitters in rat nerve terminals. An in vitro study under conditions that mimic anoxia, hypoglycemia, and ischemia. *Stroke* 1996; **27**: 941–950.
7 Dennis EA, Cao J, Hsu YH, Magrioti V, Kokotos G. Phospholipase a2 enzymes: physical structure, biological function, disease implication, chemical inhibition, and therapeutic intervention. *Chem Rev* 2011; **111**: 6130–6185.
8 Macchioni L, Corazzi L, Nardicchi V, Mannucci R, Arcuri C, Porcellati S *et al.* Rat brain cortex mitochondria release group ii secretory phospholipase a(2) under reduced membrane potential. *J Biol Chem* 2004; **279**: 37860–37869.
9 Phillis JW, Horrocks LA, Farooqui AA. Cyclooxygenases, lipoxygenases, and epoxygenases in CNS: Their role and involvement in neurological disorders. *Brain Res Rev* 2006; **52**: 201–243.
10 Bayir H, Tyurin VA, Tyurina YY, Viner R, Ritov V, Amoscato AA *et al.* Selective early cardiolipin peroxidation after traumatic brain injury: an oxidative lipidomics analysis. *Ann Neurol* 2007; **62**: 154–169.
11 Tyurina YY, Poloyac SM, Tyurin VA, Kapralov AA, Jiang J, Anthonymuthu TS *et al.* A mitochondrial pathway for biosynthesis of lipid mediators. *Nat Chem* 2014; **6**: 542–552.
12 Wipf P, Xiao J, Jiang J, Belikova NA, Tyurin VA, Fink MP *et al.* Mitochondrial targeting of selective electron scavengers: Synthesis and biological analysis of hemigramicidin-tempo conjugates. *J Am Chem Soc* 2005; **127**: 12460–12461.
13 Fink EL, Alexander H, Marco CD, Dixon CE, Kochanek PM, Jenkins LW *et al.* Experimental model of pediatric asphyxial cardiopulmonary arrest in rats. *Pediatr Crit Care Med* 2004; **5**: 139–144.
14 Perez-Pinzon MA, Stetler RA, Fiskum G. Novel mitochondrial targets for neuroprotection. *J Cereb Blood Flow Metab* 2012; **32**: 1362–1376.
15 Tyurin VA, Yanamala N, Tyurina YY, Klein-Seetharaman J, Macphee CH, Kagan VE. Specificity of lipoprotein-associated phospholipase a(2) toward oxidized phosphatidylserines: Liquid chromatography-electrospray ionization mass spectrometry characterization of products and computer modeling of interactions. *Biochemistry* 2012; **51**: 9736–9750.
16 Farooqui AA, Yang HC, Rosenberger TA, Horrocks LA. Phospholipase a2 and its role in brain tissue. *J Neurochem* 1997; **69**: 889–901.
17 Skoda EM, Davis GC, Wipf P. Allylic amines as key building blocks in the synthesis of (e)-alkene peptide isosteres. *Org Process Res Dev*2012; **16**: 26–34.
18 Ji J, Kline AE, Amoscato A, Samhan-Arias AK, Sparvero LJ, Tyurin VA *et al.* Lipidomics identifies cardiolipin oxidation as a mitochondrial target for redox therapy of brain injury. *Nat Neurosci* 2012; **15**: 1407–1413.
19 Ji J, Tyurina YY, Tang M, Feng W, Stolz DB, Clark RS *et al.* Mitochondrial injury after mechanical stretch of cortical neurons in vitro: Biomarkers of apoptosis and selective peroxidation of anionic phospholipids. *J Neurotrauma* 2012; **29**: 776–788.
20 Robinson KM, Janes MS, Beckman JS. The selective detection of mitochondrial superoxide by live cell imaging. *Nat Protoc* 2008; **3**: 941–947.
21 Fink EL, Marco CD, Donovan HA, Alexander H, Dixon CE, Jenkins LW *et al.* Brief induced hypothermia improves outcome after asphyxial cardiopulmonary arrest in juvenile rats. *Dev Neurosci* 2005; **27**: 191–199.
22 Drose S, Brandt U. Molecular mechanisms of superoxide production by the mitochondrial respiratory chain. *Adv Exp Med Biol* 2012; **748**: 145–169.
23 Tschopp J. Mitochondria: Sovereign of inflammation? *Eur J Immunol* 2011; **41**: 1196–1202.

24 Marcheselli VL, Hong S, Lukiw WJ, Tian XH, Gronert K, Musto A *et al.* Novel docosanoids inhibit brain ischemia-reperfusion-mediated leukocyte infiltration and pro-inflammatory gene expression. *J Biol Chem* 2003; **278**: 43807–43817.
25 Liu H, Rose ME, Miller TM, Li W, Shinde SN, Pickrell AM *et al.* Cox2-derived primary and cyclopentenone prostaglandins are increased after asphyxial cardiac arrest. *Brain Res* 2013; **1519**: 71–77.
26 Walton KM, DiRocco R, Bartlett BA, Koury E, Marcy VR, Jarvis B *et al.* Activation of p38mapk in microglia after ischemia. *J Neurochem* 1998; **70**: 1764–1767.
27 Zachman DK, Chicco AJ, McCune SA, Murphy RC, Moore RL, Sparagna GC. The role of calcium-independent phospholipase a2 in cardiolipin remodeling in the spontaneously hypertensive heart failure rat heart. *J Lipid Res* 2010; **51**: 525–534.
28 Malhotra A, Edelman-Novemsky I, Xu Y, Plesken H, Ma J, Schlame M *et al.* Role of calcium-independent phospholipase a2 in the pathogenesis of barth syndrome. *Proc Natl Acad Sci USA* 2009; **106**: 2337–2341.
29 Kagan VE, Tyurin VA, Jiang J, Tyurina YY, Ritov VB, Amoscato AA *et al.* Cytochrome c acts as a cardiolipin oxygenase required for release of proapoptotic factors. *Nat Chem Biol* 2005; **1**: 223–232.
30 Kagan VE, Wipf P, Stoyanovsky D, Greenberger JS, Borisenko G, Belikova NA *et al.* Mitochondrial targeting of electron scavenging antioxidants: Regulation of selective oxidation vs random chain reactions. *Adv Drug Deliv Rev* 2009; **61**: 1375–1385.
31 Liu Y, Rosenthal RE, Haywood Y, Miljkovic-Lolic M, Vanderhoek JY, Fiskum G. Normoxic ventilation after cardiac arrest reduces oxidation of brain lipids and improves neurological outcome. *Stroke* 1998; **29**: 1679–1686.
32 Akeo K, Hiramitsu T, Kanda T, Yorifuji H, Okisaka S. Comparative effects of linoleic acid and linoleic acid hydroperoxide on growth and morphology of bovine retinal pigment epithelial cells in vitro. *Curr Eye Res* 1996; **15**: 467–476.
33 Vangaveti V, Baune BT, Kennedy RL. Hydroxyoctadecadienoic acids: Novel regulators of macrophage differentiation and atherogenesis. *Ther Adv Endocrinol Metab* 2010; **1**: 51–60.

Supplementary Information accompanies the paper on the Journal of Cerebral Blood Flow & Metabolism website (http://www.nature.com/jcbfm)